A Hydrodynamic Model of Flow in Bifurcating Streams, Part 2: Effects of Environmental Thermal Differentials

W. I. A. Okuyade[1*] and T. M. Abbey[2]

[1]*Department of Mathematics and Statistics, University of Port Harcourt, Port Harcourt, Nigeria.*
[2]*Department of Physics, Applied Mathematics and Theoretical Physics Group,*
University of Port Harcourt, Port Harcourt, Nigeria.

Authors' contributions

This work was carried out in collaboration between both authors. Author TMA designed the study, wrote the protocol and supervised the work. Author WIAO managed the literature searches, solved the problem, and did the programming for the results under the guidance of author TMA. Author TMA managed the analyses of the results. Author WIAO wrote the first draft. Author TMA edited the manuscript. Both authors read and approved the final manuscript.

Original Research Article

ABSTRACT

This paper presents a hydrodynamic model of flow in a bifurcating stream, in which the effects of environmental thermal differentials are investigated. The governing nonlinear and coupled equations are solved analytically using similarity transformation and perturbation series expansions methods. Solutions for the temperature, velocity and concentration are obtained and analyzed graphically. The results show that the heat exchange parameter reduces the velocity of the flow, and this enhances early deposition of the streambed loads. Furthermore, it is seen that free convection force increases the flow velocity, thus serving as a cushion for the adverse effect of heat exchange parameter on the flow.

_____

Corresponding author: E-mail: wilsonia6011@gmail.com,
Co-author: E-mail: tamunoimi.abbey@uniport.edu.ng;

1. INTRODUCTION

Much of the studies on flow in streams and rivers have been carried out using non-hydrodynamic approaches such as hydrologic, hydraulic and stochastic probability models. The hydrologic model involves the use of spatial form of the continuity equation or water balance and flux relation Singh [1]; the hydraulic model is based on the use of St. Venant equations Singh [2]; the stochastic probability model involves the use of Monte Carlo method Hoey [3], Galino [4]. Being motivated by this, we presented an analytic and hydrodynamic model of the flow in a bifurcating stream. In the said model, which is part one of the study, the effects of bifurcation angle and nature of the source rocks on the flow were investigated, while the effects of environmental thermal differentials were played down. Presently, we shall examine the situation where the environmental thermal differentials are considered significant. Therefore, the purpose of this study is to investigate the effect of environmental thermal differentials on the flow of a bifurcating stream.

Several reports exist in literature on the flow in bifurcating and non-bifurcating channels. Bifurcation (in sense that a flow system divides into two or more daughter channels) phenomenon is seen in both natural and artificial worlds. Therefore, it is significant in science and engineering. This import greatly attracted the interest of researchers in the past decades. Pedley et al. [5] introduced the use of theoretical approach or mathematical tools in the study of branching flows. Tadjar and Smith [6] investigated a three-dimensional one-to-two symmetrical flow in which the mother is straight and of circular cross-section, containing a fully developed incident motion, while the diverging daughters are straight and of semi-circular cross-section. Using the method of direct numerical simulation and slender modeling for a variety of Reynolds number and divergent angles, they observed that a flow separation or reversal occurs at the corners of the junction. Additionally, they noticed that the inlet pressure increases as the bifurcation angle increases. Soulis [7] showed that changes in bifurcation angle alter the flow condition and changes the magnitude of the wall shear stress. Zhang et al. [8] studied the flow phenomenon in micro/mini channel networks of symmetrical bifurcation using computer simulation with analytic validation, and saw that oscillation amplitude has dominant effects on the streaming velocity in channel networks. More so, they observed that the streaming velocity is proportional to the oscillation frequency. Okuyade and Abbey [9] studied blood flow in abifurcating artery, using the method of regular perturbation, and noticed that an increase in bifurcation angle and Reynolds number increases the transport velocity factor.

The flow through porous media is prevalent in nature and artficial settings. Therefore, it is of principal interest in science and engineering. It has relevance in petroleum engineering for the study of the movement of natural gas, oil and water through the oil reserviour; in chemical engineering for filtration of and purification processes; in hydrology for studying the underground water resources. Rao and Sobha [10] investigated the flow in a rotating porous straight pipe, and showed that the Nusselt number increases with increase in porosity. Avremenko et al. [11] studied the flow in a curved porous channel with rectangular cross-section filled with a fluid saturated porous medium, the flow being driven by a constant azimuthal pressure gradient, and using a gerneralized Fourier series method of solution found that the velocity profiles depend on the geometry of the channel and Darcy number.

Moreso, the study of the flow of fluid through porous media has also been extended to include the effect of magnetic field. Abdel-Malek and Helal [12] investigated the effect of magnetic field on the flow in a rectangular enclosure using perturbation technique, and reported that the imposed magnetic field diminished the wall shear. Asadolah et al. [13] examined the influence of magnetic field on the skin friction factor of a steady fully developed laminar flow through a pipe by experimental and finite difference numerical scheme. They observed that the pressure drop varies in proportion to the square of the magnetic field and sine angle; the pressure is proportional to the flow rate, and the axial velocity asymptotically approaches its limit as the Hartmann number becomes large. Ventakaswalu et al. [14] studied the free convection flow through a vertical porous channel in the presence of an applied magnetic field using the finite difference numerical approach, and noticed that the velocity

2

decreases with the increase in the magnetic and porosity parameters throughout the region.

Similarly, magnetohydrodynamic convective heat and mass transfer in porous and non-porous media is of considerable interest in techical field due to its applications in industries, geothermal, high temperature plasma, liquid metal and MHD power generating systems. Okuyade [15] investigated the effects of magnetic field and convective force on the flow in bifurcating porous fine capillaries using the regular perturbation series expansions method, and found that magnetic field reduces the flow velocity, whereas the convective force increases it. Additionally, Okuyade and Abbey [16] examined blood flow in bifurcating arteries analytically, and observed that an increase in the heat exchange parameter and Grashof number increases the velocity, concentration and Nusselt number of the flow, while an increase in the heat exchange parameter increases the Sherwood number.

The purpose of this present paper is to examine the effects of thermal differentials on a bifurcating flowing stream.

This paper is organized in the following format: section 2 is the material and methods, section 3 is the results and discussion, and section 4 is the conclusion.

2. MATERIALS AND METHODS

There is always a temperature difference between the internal/ambient temperature of the stream and that at its surface called the external or environmental temperature condition. This temperature differential can be described in terms of the Newton's law of cooling as $\frac{\partial \theta}{\partial y} = h(\theta_{ext} - \theta_{int})$ where h is the film heat transfer coefficient that could be negative. The magnitude of the temperature at the surface of the stream is influenced by the climatic condition of the region where it is found. In particular, the environmental temperature depends tremendously on the radiation from the sun. The higher the radiation the higher it becomes. When the environmental temperature is higher than the equilibrium temperature of the stream, heat flows from the surface into it, that is, the stream absorbs heat from the environmental source. The effects of heat absorption can be seen in the energization of the water particles.

We assumed the stream bifurcates symmetrically, as shown in Fig. 1, and that the flow is symmetrical about the z'-axis. Therefore, if (u', v') are respectively the velocity components of the fluid in the mutually orthogonal (x', y') axes, then the mathematical equations of mass balance/continuity, momentum, energy and diffusion governing the flow, considering the Boussinesq approximations, become:

$$\frac{\partial u'}{\partial x'} + \frac{\partial v'}{\partial y'} = 0 \tag{1}$$

$$u'\frac{\partial u'}{\partial x'} + v'\frac{\partial u'}{\partial y'} = -\frac{1}{\rho'}\frac{\partial p'}{\partial x'} + \frac{\mu}{\rho'}\left(\frac{\partial^2 u'}{\partial x'^2} + \frac{\partial^2 u'}{\partial y'^2}\right)$$
$$+ g\beta_t\left(T' - T_\infty\right) + g\beta_c\left(C' - C_\infty\right) - \frac{\sigma_e B_o^2 u'}{\rho'^2 \mu_m} - \frac{\upsilon u'}{\kappa} \tag{2}$$

$$u'\frac{\partial v'}{\partial x'} + v'\frac{\partial v'}{\partial y'} = -\frac{1}{\rho'}\frac{\partial p'}{\partial y'} + \frac{\mu}{\rho'}\left(\frac{\partial^2 u'}{\partial x'^2} + \frac{\partial^2 u'}{\partial y'^2}\right) \tag{3}$$

$$u'\frac{\partial T'}{\partial x'} + v'\frac{\partial T'}{\partial y'} = -\frac{1}{\rho'}\frac{k_o}{C_p}\left(\frac{\partial^2 T'}{\partial x'^2} + \frac{\partial^2 T'}{\partial y'^2}\right) + \frac{1}{\rho'}\frac{Q}{C_p}\left(T' - T_\infty\right) \tag{4}$$

$$u\frac{\partial C'}{\partial x'} + v'\frac{\partial C'}{\partial y'} = -\frac{D}{\rho'}\left(\frac{\partial^2 C'}{\partial x'^2} + \frac{\partial^2 C'}{\partial y'^2}\right) + \frac{k_r^2}{\rho'}\left(C' - C_\infty\right) \tag{5}$$

The model examines the dynamics of a bifurcating stream flowing from a point $x' = -\infty$ towards a shore at $x' = x_o$, then continued towards $x' = +\infty$, as seen in Fig. 1. The model shows that the channel is assumed symmetrical and divided into two regions: the upstream (or mother) region $x' < x_o$ and downstream (or daughter) region $x' > x_o$, where x_o is the bifurcation or the nodal point, which is assumed the origin such that the stream boundaries become $y' = \pm d$ for the upstream region and $y' = \alpha x'$ for the downstream region. Due to the geometrical transition between the mother and daughter channels, the problem of wall curvature effect is bound to occur. To fix up this, a very
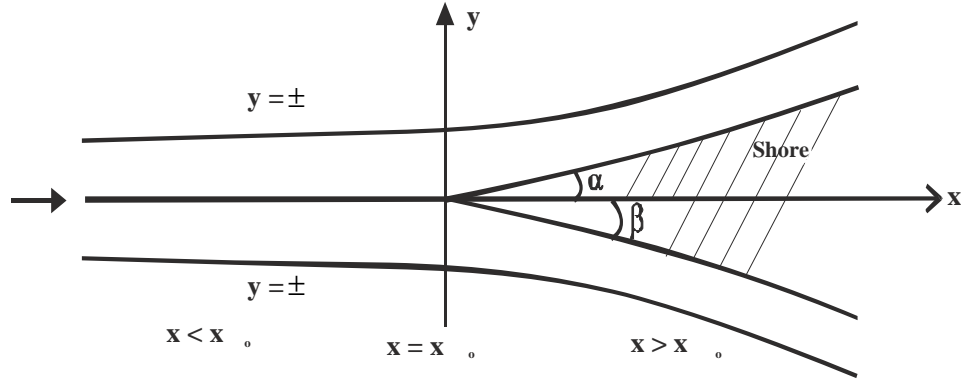
Fig. 1. A physical model of symmetrical bifurcating flowing stream (α and β are the bifurcation angles and are equal)

simple transition wherein the width of the daughter channel is made equal to half that of the mother channel i.e. $\pm d$ is such that the variation of the bifurcation angle is straight-forwardly used (see Tadjar and Smith [6]). Furthermore, if the width of the stream ($2d$) is far less than its length (l_o) before the point of bifurcation such that the ratio of $\dfrac{2d}{l_o} = \Re \ll 1$, (where $\Re$ is the aspect ratio), the flow is laminar and Poiseuille (see Bestman [17]). d is assumed to be non-dimensionally equal to one (see Tadjar and Smith [6]). Similarly, at the entry region of the mother channel, the flow velocity is given as $u' = U_o(1 - y'^2)$, where U_o is the characteristic velocity, which is taken to be maximum at the centre and zero at the wall (see Tadjar and Smith [6]). Based on the fore-going, the boundary conditions are:

$$u'=1, v'=0, T'=1, C'=1 \ \text{ at } \ y'=0 \qquad (6)$$

$$u'=0, v'=0, T'=T_w, C'=C_w \ \text{ at } \ y'=1 \qquad (7)$$

for the mother channel

$$u'=0, v'=0, T'=0, C'=0 \ \text{ at } \ y'=0 \qquad (8)$$

$$u'=0, v'=0, T'=\gamma_1 T_w, C'=\gamma_2 C_w, \ \gamma_1 < 1,$$
$$\gamma_2 < 1 \ \text{ at } \ y'=\alpha x' \qquad (9)$$

for the daughter channel

Introducing the dimensionless variables and similarity transformations,

We have

$$f'' = 0 \qquad (10)$$

$$f''' + f'' - M_1^2 f' + \text{Re}(f'f'' + ff''') = -Gr\,\Theta - Gc\,\Phi \qquad (11)$$

$$\Theta'' + \Theta' + \text{Re}\,\text{Pr}(-f'\Theta + f\Theta') + N^2\Theta = 0 \qquad (12)$$

$$\Phi'' + \Phi' + Re\,Sc(-f'\Phi' + f\Phi') + \delta_1^2\Phi = 0 \qquad (13)$$

with the boundary indications:

$$f=1, f'=0, \Theta=1, \Phi=1 \ \text{ at } \ \eta=0 \qquad (14)$$

$$f'=0, f=0, \Theta=\Theta_w, \Phi=\Phi_w \ \text{ at } \ \eta=1 \qquad (15)$$

for the mother channel

$$f=0, f'=0, \Theta=0, \Phi=0 \ \text{ at } \ \eta=0 \qquad (16)$$

$$f'=0, f=0, \Theta=\gamma_1\Theta_w, \Phi=\gamma_2\Phi_w,$$
$$\gamma_1 < 1, \gamma_2 < 1 \ \text{ at } \ \eta=ax \qquad (17)$$

for the daughter channel

where

$$M_1^2 = (\chi^2 + M^2)$$

$$x = \frac{x'}{l_c}, \quad y = \frac{y'}{l_c}, \quad u = \frac{u'}{U_o}, \quad v = \frac{v'}{U_o}, \quad p = \frac{p'}{p_\infty}, \quad \rho = \rho' U_o^2, \Theta = \frac{T'-T_\infty}{T_w - T_\infty}, \Phi = \frac{C'-C_\infty}{C_w - C_\infty},$$

$$\upsilon = \frac{\mu}{\rho}, \mathrm{Re} = \frac{\rho U_o l_c}{\mu}, \quad Gr = \frac{\rho g \beta_t (T_w - T_\infty) l_c^2}{\mu U_o}, \quad Gc = \frac{\rho g \beta_c (C_w - C_\infty) l_c^2}{\mu U_o}, \chi^2 = \frac{l_c^2}{\kappa},$$

$$\delta_1^2 = \frac{k_r^2 l_c^2}{D}, \quad M^2 = \frac{\sigma_e B_o^2 l_c^2}{\rho \mu \mu_m}, \quad N^2 = \frac{\mu C_p l_c^2}{k_o}, \quad Sc = \frac{\mu}{\rho D}$$

are the dimensionless variables,

$$\Psi = (U_o \upsilon \ x)^{\frac{1}{2}} f(\eta), \quad \eta = \left(\frac{U_o}{\upsilon x}\right)^{1/2} y \quad (18)$$

the similarity transformations,

$$u = \frac{\partial \Psi}{\partial y}, \quad v = -\frac{\partial \Psi}{\partial x} \quad (19)$$

the velocity components,

and β_t and β_c are the volumetric expansion coefficient for temperature and concentration respectively; p' is the pressure; C_∞ is the concentration at equilibrium. T_∞ is the temperature at equilibrium; κ is the permeability parameter of the porous medium. B_o^2 is the applied uniform magnetic field strength due to the nature of the fluid; σ_e is the electrical conductivity of the fluid; k_o is the thermal conductivity of the fluid. C_p is the specific heat capacity at constant pressure; Q is the heat absorption coefficient; k_r^2 is the rate of chemical reaction of the fluid, which is homogeneous and of order one. C' is concentration (quantity of material being transported); D diffusion coefficient; **g** is gravitational field vector; T' is the fluid temperature; ρ' is the density of the fluid. μ is the viscosity of the fluid; μ_m is the magnetic permeability of the fluid; υ is the kinematic viscosity; ℓ_c is the scale length; U_o is the characteristic or reference velocity which is maximum at the centre and almost zero at the wall. C_w is the constant wall concentration at

which the channel is maintained; T_w is the constant wall temperature at which the channel is maintained; p_∞ is the ambient/equilibrium pressure. Re is the Reynolds number; Gr is the Grashof number due to temperature difference; Gc is the Grashof number due to concentration difference. χ^2 is the local Darcy number; M^2 is the Hartmann's number; Pr is the Prandtl number; Sc is the Schmidt number; δ_1^2 is the rate of chemical reaction; and N^2 is the heat exchange parameter.

Equations (10) - (13) are coupled and highly non-linear. Therefore, to linearize and make them tractable, we introduce the regular perturbation series solutions of the form:

$$h(x,y) = h_o(x,y) + \xi h_1(x,y) + \dots \quad (20)$$

where $\xi = \dfrac{1}{\mathrm{Re}} << 1$ Is the perturbing parameter.

We choose this parameter because, almost at the point of bifurcation, due to a change in the geometrical configuration, the inertial force rises and the momentum increases. The increase in the momentum is associated with a drastic increase in the Reynolds number, indicating a sort of turbulent flow. In this regard, equations (10) - (17) become:

for the zeroth order:

$$f_o'' = 0 \quad (21)$$

$$f_o''' + f_o'' - M_1^2 f_o' = -Gr\Theta_o - Gc\Phi_o \quad (22)$$

$$\Theta_o'' + \Theta_o' + N^2 \Theta_o = 0 \quad (23)$$

$$\Phi_o'' + \Phi_o' + \delta_1^2 \Phi_o = 0 \quad (24)$$

with the boundary conditions

$$f_o = 1, f_o^{'} = f_o^{''} = 0, \Theta_o = 1, \Phi_o = 1 \quad \text{at} \; \eta = 0 \tag{25}$$

$$f_o = 0, f_o^{'} = f_o^{''} = 0, \Theta_o = \Theta_w, \Phi_o = \Phi_w \; \text{at} \; \eta = 1 \tag{26}$$

for the first order:

$$f_{1,}^{''} = 0 \tag{27}$$

$$f_1^{'''} + f_1^{''} - M_1^2 f_1^{'} = f_o^{'} f_o^{''} - f_o f_o^{''} - Gr\Theta_1 - Gc\Phi_1 \tag{28}$$

$$\Theta_1^{''} + \Theta_1^{'} + N^2 \Theta_1 = \Pr(f_o^{'} \Theta_o^{'} - f_o \Theta_o^{'}) \tag{29}$$

$$\Phi_1^{''} + \Phi_1^{'} + \delta_1^2 \Phi_1 = Sc(f_o^{'} \Phi_o^{'} - f_o \Phi_o^{'}) \tag{30}$$

with the boundary conditions

$$f_1 = 0, f_1^{'} = 0, \Theta_1 = 0, \Phi_1 = 0 \quad \text{at} \; \eta = 0 \tag{31}$$

$$f_1 = 0, f_1^{'} = 0, \Theta_1 = \gamma_1 \Theta_w, \Phi_1 = \gamma_2 \Phi_w,$$
$$\gamma_1 < 1, \gamma_2 < 1 \quad \text{at} \; \eta = ax \tag{32}$$

The zeroth order equations describe the flow in the upstream channel, while the first order equations describe the flow in the downstream channels. The presence of the zeroth order terms in the first order equations indicate the influence of the upstream on the downstream flow.

The solutions to equations (21) - (26) and (27) - (32) are:

$$\Theta_o(\eta) = \frac{\Theta_w e^{\frac{1}{2}(1-\eta)} \sinh\mu_1\eta}{\sinh\mu_1} + \frac{e^{-\frac{1}{2}(1-\eta)} \sinh\mu_1(1-\eta)}{\sinh\mu_1} \tag{33}$$

$$\Phi_o(\eta) = \frac{\Phi_w e^{\frac{1}{2}(1-\eta)} \sinh\mu_2\eta}{\sinh\mu_2} + \frac{e^{-\frac{1}{2}(1-\eta)} \sinh\mu_2(1-\eta)}{\sinh\mu_2} \tag{34}$$

$$f_o(\eta) = \frac{\left(f_{o(p)}(0)e^{-(\mu 3 + \eta/2)} \sinh\mu_3\eta\right)}{\sinh\mu_3} + \frac{\left(f_{o(p)}(1)e^{-1/2(1-\eta)} \sinh\mu_3\eta\right)}{\sinh\mu_3}$$
$$- f_{o(p)}(0)e^{-(\mu_3 + \eta/2)} + f_{o(p)}(\eta) \tag{35}$$

for the mother channel

$$\Theta_1(\eta) = \frac{\gamma_1 \Theta_w e^{\frac{1}{2}(\alpha x - \eta)} \sinh\mu_1\eta}{\sinh(\mu_1 \alpha x)} - \frac{\Theta_{1(p)}(\alpha x)e^{-\frac{1}{2}(\alpha x - \eta)} \sinh\mu_1\eta}{\sinh(\mu_1 \alpha x)}$$
$$+ \frac{\Theta_{1(p)}(0)e^{-(\mu\alpha x + \eta/2)} \sinh\mu_1\eta}{\sinh(\mu_1 \alpha x)} - \Theta_{1(p)}(0)e^{-(\alpha x - (\mu_1 + 1/2)\eta)} + \Theta_{1(p)}(\eta) \tag{36}$$

$$\Phi_1(\eta) = \frac{\gamma_2 \Phi_w e^{\frac{1}{2}(\alpha x - \eta)} \sinh\mu_2\eta}{\sinh(\mu_2 \alpha x)} + \frac{\Phi_{1(p)}(\alpha x)e^{-\frac{1}{2}(\alpha x - \eta)} \sinh\mu_2\eta}{\sinh(\mu_2 \alpha x)}$$
$$+ \frac{\Phi_{1(p)}(0)e^{-(\mu\alpha x + \eta/2)} \sinh\mu_2\eta}{\sinh(\mu_2 \alpha x)} - \Phi_{1(p)}(0)e^{-(\alpha x - (\mu_2 + 1/2)\eta)} + \Phi_{1(p)}(\eta) \tag{37}$$

$$f_1(\eta) = \frac{f_{1(p)}(0)e^{-(\mu_3\alpha x+\eta/2)}\sinh\mu_3\eta}{\sinh\mu_3\alpha x} + \frac{f_{1(p)}(\alpha x)e^{1/2(\alpha x-\eta)}\sinh\mu_3\eta}{\sinh(\mu_3\alpha x)}$$

$$-f_{1(p)}(0)e^{(\alpha x-(\mu_{3+1/2})\eta)} + f_{1(p)}(\eta) \tag{38}$$

and for the daughter region.

3. RESULTS AND DISCUSSION

This paper investigates the effects of thermal differentials on the flow in a bifurcating stream. To this end, Fig. 2 – Fig. 8 obtained using Maple 12 computational soft ware show the profiles of the flow variables obtained for various values of χ_1^2, N^2 and Gr/Gc. For realistic values of Pr =0.71, γ_1 = 0.6, γ_2 =0.6, γ =0.7, Φ_w = 2.0, Θ_w =2.0, $\delta_1^2 = 0.2$, M^2= 0.2, α =10, Re=400, and varying values of χ^2 = 0.1, 0.5, 1.0, 10; N^2= 0.001, 0.01, 0.1, 0.4 and Gr/Gc=0.01, 0.1, 0.5, 1.0, 5, 10, the profiles indicate that the flow velocity decreases as χ^2 and N^2 increase, but increases with the increase in Gr/Gc.

A high porosity of the stream bank may give room for a soak-away of the water. Therefore, as the porosity increases the stream water is soaked away into its bank, thus leading to a dcreases in its volume. Moreso, the water level of the stream will remain decreased if there is not a commensurate increase in the water supplied from the aquifers that feed it, possibly, due to man's water delivery activities on them. Consequent upon these, the flow velocity, which is usually maximum when the volume is high,

decreases. These may account for what is seen in Fig. 2. And, this is in perfect agreement with Avremenko et al. [11], Asadolah et al. [13] and Ventakaswalu et al. [14]. s In another development, a high porosity of the source rock of the stream creates room for water to flow from the supplying aquifers into it. However, by the analysis of this model the flow velocity of the water from the aquifers decreases with high porosity of the source rock. Even so, the oscillatory/fluctuation motion, manifested in the form of back-and-forth movement of the water, as seen in Fig. 3 and Fig. 4, possibly, may be due to the internal waves developed in the water in the flow process, or may be due to the interaction between the pressure forces and the gravity forces.

Furthermore, as the environmental temperature increases, the stream may lose its water through evaporation, and soak-away into the dry flood plain. This leads to a decrease in its water level. Again, if the water supplied from the aquifers is not equatable to that which is lost (due to man's water delivery activities on them), the stream water level in such a season remains reduced. Consequently, the velocity, which is usually maximum when the water volume is high, drops. This accounts for the results seen in Fig. 5.
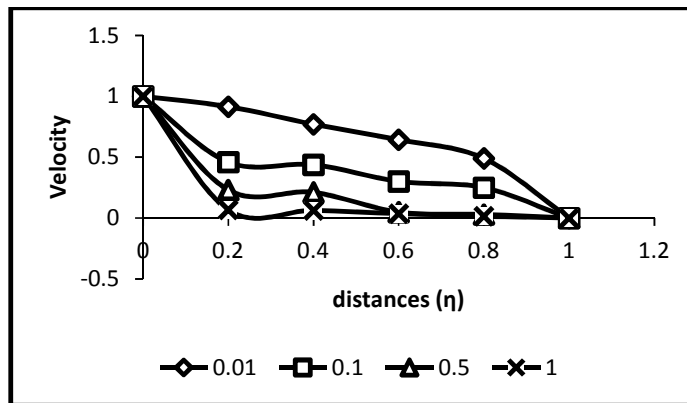

Fig. 2. Velocity-porosity parameter (χ^2) profiles at various distances (η) in the mother channel
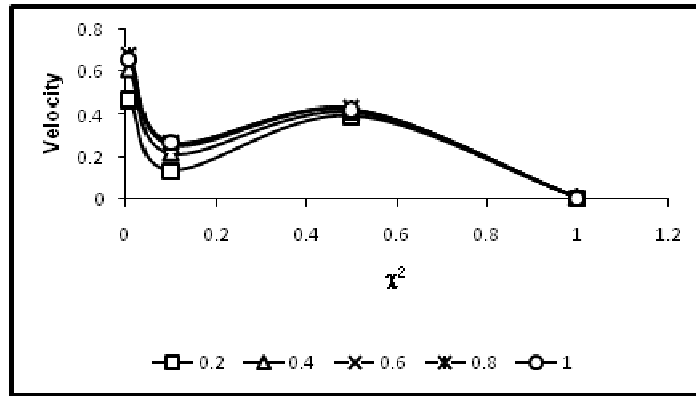
Fig. 3. Velocity profiles for various porosity parameter (χ^2) in the daughter channel
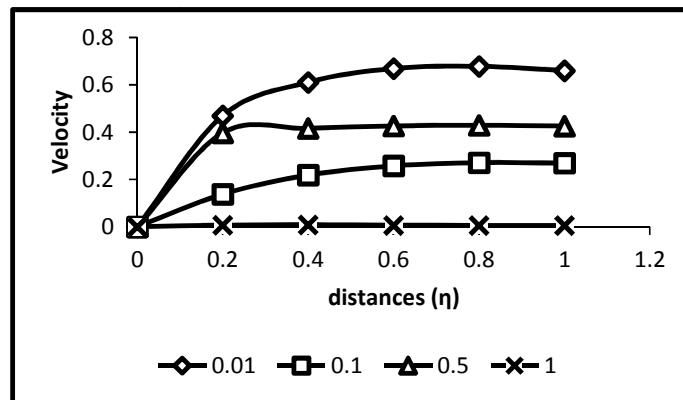

Fig. 4. Velocity-porosity parameter (χ^2) profiles at various distances (η) in the daughter channel
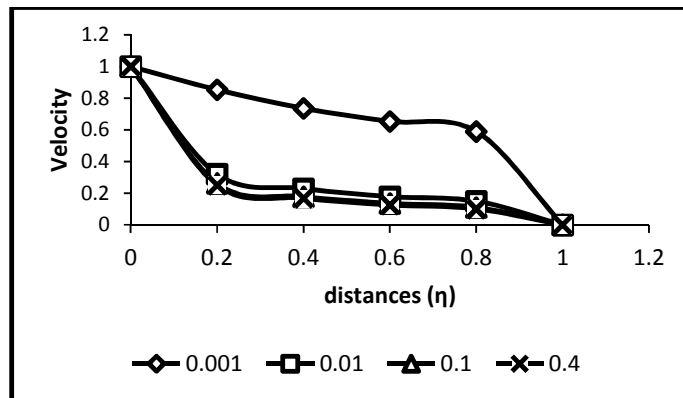

Fig. 5. Velocity-heat exchange parameter (N^2) profiles at various distances (η) in the mother channel

On the other hand, there is always a temperature differential between the environmental temperature and the ambient temperature of the water.The temperature differential in the presence of gravity produces free convection currents, which serve as lifting/buoyancy forces for the water particles. In particular, the temperature differential depends on the environmental temperature, which in turn depends on the radiation from the sun. The higher the radiation, the higher the temperature differential, and the higher the convection currents, otherwise called buoyancy force or Grashof number (which in this case is due to temperature change) produced. The increase in the buoyancy force increases the flow velocity

(see Fig. 6–Fig. 8). A comparison with previous research works shows a complete agreement; see Okuyade [15], Okuyade and Abbey [16].

The increase and decrease in the velocity coupled with the oscillating/fluctuating motion of the water have some great significance on the flow. The increase in velocity saves the stream from early shallow-up as it tends to delay the deposition of the sediments and bedloads it is carrying in its course towards the standing water bodies into which it empties its water. On the other hand, the decrease in velocity produces the contrary situation. Furthermore, the oscillatory/fluctuating motion leads to loss of energy for the flow in the axial direction, and this adversely affects the transport of the bedloads.
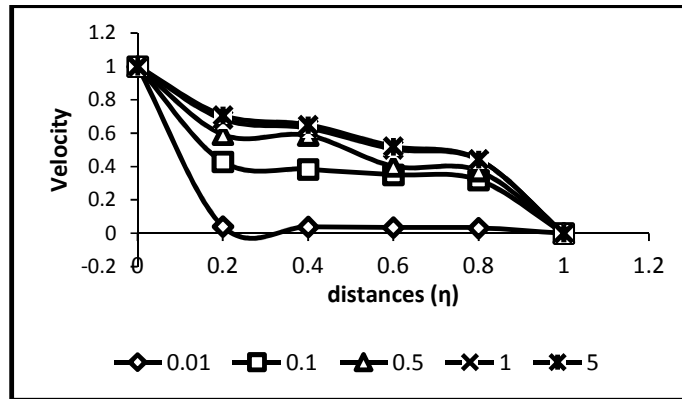

Fig. 6. Velocity-Grashof number (Gr/Gc) profiles at various distances (η) in the mother channel
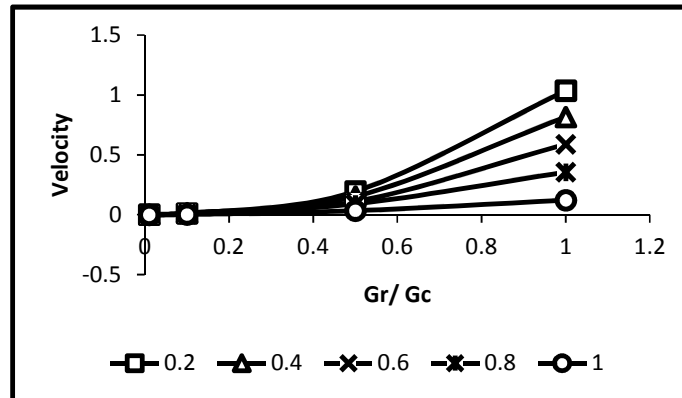

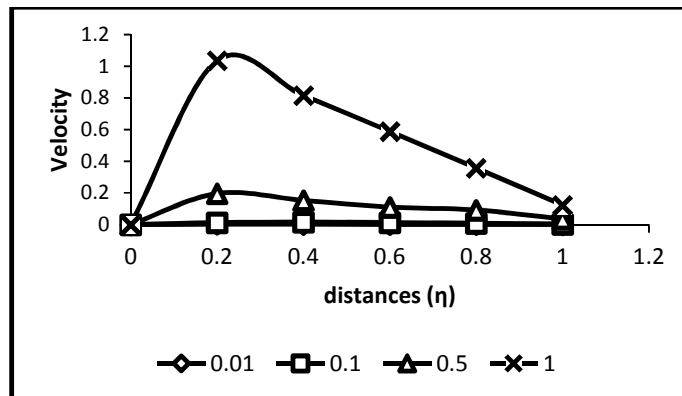**Fig. 7. Velocity profiles for various Grashof numbers (Gr/Gc) in the daughter channel**

Fig. 8. Velocity-Grashof numbers (Gr/Gc) profiles at various distances (η) in the daughter channel

9

4. CONCLUSION

The steady flow in a bifurcating stream with emphasis on the effects of environmental thermal differentials is presented. The solutions of the problem are analyzed graphically. The analyses show that the porosity and heat exchange parameters decrease the flow velocity, while the free convection force increases it. Furthermore, an increase in the porosity leads to a oscillatory fluctuating motion. These results have serious implications on the flow. The increase in velocity tends to delay the deposition of sediments/ bedloads on the stream floor and flood plains, thus saving it from early shallow-up. On the other hand, the decrease in the velocity leads to the contrary. Similarly, the fluctuating motion leads to loss of energy for the axial flow. In particular, the free convection force tends to cushion the velocity reducing-effects of porosity and heat exchange parameters. It is worthy to note that a considerable amount of work is needed to further study and understand the streaming flow hydrodynamically.

COMPETING INTERESTS

Authors have declared that no competing interests exist.

REFERENCES

1. Singh VP. Hydrologic systems: Rainfall-run-off modeling. New Jessey: Prentice House Englewood Cliffs. 1988;1.
2. Singh VP. Kinematic wave modeling in water resources, surface water hydrology. New York: John Wiley and Sons; 1996.
3. Hoey T. Temporal variations in bed load transport rate and sediment storage in gravel-bed rivers. Prog. Physical Geography. 1992;16(3):319–38.
4. Marusic Galino. A study on the mathematical modeling of water quality in river-type aquatic system. WSEAS Transactions on Fluid Mechanics. 2013; 80–9.
5. Pedley TJ, Schroter RC, Sudlow MF. The prediction of pressure drop and variation of resistance within the human bronchial airways. Resp. Physiology. 1970;9:387–405.
6. Tadjfar M, Smith FT. Direct simulation and modeling of a 3-dimensional bifurcating tube flow. J Fluid Mechanics. 2004;519:1-32.
7. Soulis. J Biomech. 2004;39:742–49.
8. Zhang Z, Fadl A, Liu C, Meyer DML. Fluid streaming in micro/ mini-bifurcating networks. J Fluid Engineering, ASME. 2009;131:084501-8.
9. Okuyade WIA, Abbey TM. Analytic study of blood flow in bifurcating arteries, part 1-effects of bifurcating angle and magnetic field. International Organization of Scientific Research J Mathematics. 2015;(I.D: G54040 - in press).
10. Rao Ramana VV, Sobha VV. Heat transfer of a saturated porous flow in a rotating straight pipe. Proceeding of the Tenth National Heat and Mass Transfer Conference, Madurai Kamoraj University, Madurai. 1987;13.
11. Avramenko AA, Kuznetsov AV. Flow in a curved porous channel with rectangular cross-section. J Porous Media. 2008;241-48.
    DOI: 10.1615/JporMedia.v.11.i3.20
12. Abdel-Malek MB, Helal MM. Similarity solutions for magneto-force unsteady free convective laminar boundary–layer flow.J Comput. App. Maths. 2008;218:202–14.
13. Asadolah, Malekzadeh, Amir Heydarinasab, Bahram Dabir. Magnetic field effect on fluid flow characteristics in a pipe for laminar flow. J Mechanical Sci. and Tech. 2011;25:333-39.
14. Venkateswalu S, Suryanarayama Rao KV, Rambupal Reddy B. Finite difference analysis on convective heat transfer flow through porous medium in a vertical channel with magnetic field. Indian Journal of Applied Maths and Mechanics. 2011; 7(7):74–94.
15. Okuyade WIA. MHD blood flow in bifurcating porous fine capillaries. African J Science Research. 2015;4(4):56-59.
16. Okuyade WIA, Abbey TM. Analytic study of blood flow in bifurcating arteries, part 2- effects of environmental temperature differentials. International Organization of Scientific Research J Mechanical Engineering. 2015;(I.D: G54083 - in press).
17. Bestman AR. Global models for the biomechanics of green plants, part 1. International J Energy Research. 1991;16: 677– 84.

APPENDICES

$$f_{o(p)}(\eta) = -\left(\frac{n_3}{n_3\left(n_3^2 - n_2 n_3\right)} - \frac{1}{\left(n_3^2 - n_2 n_3\right)} \right) \left(\frac{GrAe^{\lambda_1\eta}}{\lambda_1} + \frac{GrBe^{\lambda_2\eta}}{\lambda_2} + \frac{GrCe^{m_1\eta}}{m_1} + \frac{GrDe^{m_2\eta}}{m_2} \right)$$

$$+ \frac{n_3}{n_3\left(n_3^2 - n_2 n_3\right)} \left(\frac{GrAe^{\lambda_1\eta}}{\left(\lambda_1 - n_2\right)} + \frac{GrBe^{\lambda_2\eta}}{\left(\lambda_2 - n_2\right)} + \frac{GrCe^{m_1\eta}}{\left(m_1 - n_2\right)} + \frac{GrDe^{m_2\eta}}{\left(m_2 - n_2\right)} \right)$$

$$- \frac{1}{n_3\left(n_3^2 - n_2 n_3\right)} \left(\frac{GrAe^{\lambda_1\eta}}{\left(\lambda_1 - n_3\right)} + \frac{GrBe^{\lambda_2\eta}}{\left(\lambda_2 - n_3\right)} + \frac{GrCe^{m_1\eta}}{\left(m_1 - n_3\right)} + \frac{GrDe^{m_2\eta}}{\left(m_2 - n_3\right)} \right)$$

$$\lambda_1 = -\frac{1}{2} + \frac{\sqrt{1 - 4N^2}}{2}, \ \lambda_2 = -\frac{1}{2} - \frac{\sqrt{1 - 4N^2}}{2}$$

$$\lambda_1 = -\frac{1}{2} + \mu_1, \ \lambda_2 = -\frac{1}{2} - \mu_1, \ \mu_1 = \frac{\sqrt{1 - 4N^2}}{2}$$

$$m_1 = -\frac{1}{2} + \mu_2, \ m_2 = -\frac{1}{2} - \mu_2, \ \mu_2 = \frac{\sqrt{1 - 4\delta_1^2}}{2}$$

$$n_2 = -\frac{1}{2} + \mu_3, \ n_3 = -\frac{1}{2} - \mu_3, \ \mu_3 = \frac{\sqrt{1 - 4M^2}}{2}$$

$$A = \frac{\Theta_w e^{1/2} - e^{\mu_1}}{\sinh \mu_1}, \ B = \frac{e^{\mu_1} - \Theta_w e^{1/2}}{\sinh \mu_1}, \ C = \frac{\Phi_w e^{1/2} - e^{\mu_2}}{\sinh \mu_2}, \ D = \frac{e^{\mu_2} - \Phi_w e^{1/2}}{\sinh \mu_2}$$

$$\Theta_{1(p)}(\eta) = \frac{\Pr}{\left(\lambda_2 - \lambda_1\right)} \Big[\ \lambda_1 FAe^{(\lambda_1 + n_2)\eta} + \lambda_1 GAe^{(\lambda_1 + n_3)\eta}$$

$$- \left(\frac{n_3}{n_2\left(n_3^2 - n_2 n_3\right)} - \frac{1}{\left(n_3^2 - n_2 n_3\right)} \right) \left(\begin{array}{l} GrA^2 e^{2\lambda_1\eta} + \dfrac{\lambda_1 GrABe^{(\lambda_1 + \lambda_2)\eta}}{\lambda_2} + \dfrac{\lambda_1 GcACe^{(\lambda_1 + m_1)\eta}}{m_1} \\[3mm] + \dfrac{\lambda_1 GcADe^{(\lambda_1 + m_2)\eta}}{m_2} \end{array} \right)$$

$$+ \frac{n_3}{n_2\left(n_3^2 - n_2 n_3\right)} \left(\frac{\lambda_1 GrA^2 e^{2\lambda_1\eta}}{\left(\lambda_1 - n_2\right)} + \frac{\lambda_1 GrABe^{(\lambda_1 + \lambda_2)\eta}}{\left(\lambda_2 - n_2\right)} + \frac{\lambda_1 GcACe^{(\lambda_1 + m_1)\eta}}{\left(m_1 - n_2\right)} + \frac{\lambda_1 GcADe^{(\lambda_1 + m_2)\eta}}{\left(m_2 - n_2\right)} \right)$$

$$-\frac{1}{\left(n_3^2-n_2n_3\right)}\left(\frac{\lambda_1 GrA^2 e^{2\lambda_1\eta}}{\left(\lambda_1-n_3\right)}+\frac{\lambda_1 GrABe^{(\lambda_1+\lambda_2)\eta}}{\left(\lambda_2-n_3\right)}+\frac{\lambda_1 GcACe^{(\lambda_1+m_1)\eta}}{\left(m_1-n_3\right)}+\frac{\lambda_1 GcADe^{(\lambda_1+m_2)\eta}}{\left(m_2-n_3\right)}\right)\ ]+...$$

$$\Phi_{1(p)}(\eta)=\frac{Sc}{\left(m_2-m_1\right)}[\ \ m_1 FCe^{(m_1+n_2)\eta}+m_1 GCe^{(m_1+n_3)\eta}$$

$$-\left(\frac{n_3}{n_2\left(n_3^2-n_2n_3\right)}-\frac{1}{\left(n_3^2-n_2n_3\right)}\ \right)\left(\begin{array}{l}\dfrac{m_1 GrACe^{(\lambda_1+m_1)\eta}}{\lambda_1}+\dfrac{m_1 GrBCe^{(\lambda_2+m_1)\eta}}{\lambda_2}+GcC^2 e^{2m_1\eta}\\[2ex]+\dfrac{m_1 GcCDe^{(m_1+m_2)\eta}}{m_2}\end{array}\right)$$

$$+\frac{n_3}{n_2\left(n_3^2-n_2n_3\right)}\left(\frac{m_1 GrACe^{(\lambda_1+m_1)\eta}}{\left(\lambda_1-n_2\right)}+\frac{m_1 GrBCe^{(\lambda_2+m_1)\eta}}{\left(\lambda_2-n_2\right)}+\frac{m_1 GcC^2 e^{2m_1\eta}}{\left(m_1-n_2\right)}+\frac{m_1 GcCDe^{(m_1+m_2)\eta}}{\left(m_2-n_2\right)}\right)$$

$$-\frac{1}{\left(n_3^2-n_2n_3\right)}\left(\frac{m_1 GrACe^{(\lambda_1+m_1)\eta}}{\left(\lambda_1-n_3\right)}+\frac{m_1 GrBCe^{(\lambda_2+m_1)\eta}}{\left(\lambda_2-n_3\right)}+\frac{m_1 GcC^2 e^{2m_1\eta}}{\left(m_1-n_3\right)}+\frac{m_1 GcCDe^{(m_1+m_2)\eta}}{\left(m_2-n_3\right)}\right)\ ]+...$$

$$-Gr\ \left\{\frac{J_1 e^{n_1\eta}}{n_2}+\frac{J_2 e^{n_2\eta}}{n_2}\ \ +\frac{Pr}{\left(\lambda_2-\lambda_1\right)}\left[\frac{\lambda_1 FAe^{(\lambda_1+n_2)\eta}}{\left(\lambda_1+n_2\right)}+\frac{\lambda_1 GAe^{(\lambda_1+n_3)\eta}}{\left(\lambda_1+n_3\right)}\right.\right.$$

$$-\left(\frac{n_3}{\left(n_3^2-n_2n_3\right)}-\frac{1}{\left(n_3^2-n_2n_3\right)}\right)\left(\frac{GrA^2 e^{2\lambda_1\eta}}{2}+\frac{GrBAe^{(\lambda_1+\lambda_2)\eta}}{\left(\lambda_1+\lambda_2\right)}+\frac{\lambda_1 GcCAe^{(\lambda_1+m_1)\eta}}{\left(\lambda_1+m_1\right)m_1}+\frac{\lambda_1 GcDAe^{(\lambda_1+m_2)\eta}}{\left(\lambda_1+m_2\right)m_2}\right)$$

$$+\frac{n_3}{n_2\left(n_3^2-n_2n_3\right)}\left(\frac{GrA^2 e^{2\lambda_1\eta}}{2\left(\lambda_1-n_2\right)}+\frac{\lambda_1 GrBAe^{(\lambda_1+\lambda_2)\eta}}{\left(\lambda_2-n_2\right)\left(\lambda_1+\lambda_2\right)}+\frac{\lambda_1 GcCAe^{(\lambda_1+m_1)\eta}}{\left(m_1-n_2\right)\left(\lambda_1+m_1\right)}+\frac{\lambda_1 GcDAe^{(\lambda_1+m_2)\eta}}{\left(m_2-n_2\right)\left(\lambda_1+m_2\right)}\right)$$

$$-\frac{1}{\left(n_3^2-n_2n_3\right)}\left(\frac{GrA^2 e^{2\lambda_1\eta}}{2\left(\lambda_1-n_3\right)}+\frac{\lambda_1 GrBAe^{(\lambda_1+\lambda_2)\eta}}{\left(\lambda_2-n_3\right)\left(\lambda_1+\lambda_2\right)}+\frac{\lambda_1 GcCAe^{(\lambda_1+m_1)\eta}}{\left(m_1-n_3\right)\left(\lambda_1+m_1\right)}+\frac{\lambda_1 GcDAe^{(\lambda_1+m_2)\eta}}{\left(m_2-n_3\right)\left(\lambda_1+m_2\right)}\right)\ ]+...\}$$

$$f_{1(p)}(\eta)=\left(\frac{n_3}{n_2\left(n_3^2-n_2n_3\right)}-\frac{1}{\left(n_3^2-n_2n_2\right)}\right)\left\{\ \left[Fe^{n_2\eta}+Ge^{n_3\eta}\right.\right.$$

$$-\left(\frac{n_3}{n_2\left(n_3^2-n_2n_3\right)}-\frac{1}{\left(n_3^2-n_2n_3\right)}\ \right)\left(\frac{GrAe^{\lambda_1\eta}}{\lambda_1}+\frac{GrBe^{\lambda_2\eta}}{\lambda_2}+\frac{GcCe^{m_1\eta}}{m_1}+\frac{GcDe^{m_2\eta}}{m_2}\right)$$

$$+\frac{n_3}{n_2\left(n_3^2-n_2n_3\right)}\left(\frac{GrAe^{\lambda_1\eta}}{\left(\lambda_1-n_2\right)}+\frac{GrBe^{\lambda_2\eta}}{\left(\lambda_2-n_2\right)}+\frac{GcCe^{m_1\eta}}{\left(m_1-n_2\right)}+\frac{GcDe^{m_2\eta}}{\left(m_2-n_2\right)}\right)$$

$$-\frac{1}{\left(n_3^2-n_2n_3\right)}\left(\frac{GrAe^{\lambda_1\eta}}{\left(\lambda_1-n_3\right)}+\frac{GrBe^{\lambda_2\eta}}{\left(\lambda_2-n_3\right)}+\frac{GcCe^{m_1\eta}}{\left(m_1-n_3\right)}+\frac{GcDe^{m_2\eta}}{\left(m_2-n_3\right)}\right)\quad]+...$$

$$-\frac{1}{\left(n_3^2-n_2n_3\right)}\left(\frac{GrAe^{\lambda_1\eta}}{\left(\lambda_1-n_3\right)}+\frac{GrBe^{\lambda_2\eta}}{\left(\lambda_2-n_3\right)}+\frac{GcCe^{m_1\eta}}{\left(m_1-n_3\right)}+\frac{GcDe^{m_2\eta}}{\left(m_2-n_3\right)}\right)\quad]$$

$$-\left(\frac{n_3}{\left(n_3^2-n_2n_3\right)}-\frac{1}{\left(n_3^2-n_2n_3\right)}\right)\left(\frac{GrA^2e^{2\lambda_1\eta}}{2}+\frac{GrBAe^{(\lambda_1+\lambda_2)\eta}}{\left(\lambda_1+\lambda_2\right)}+\frac{\lambda_1GcCAe^{(\lambda_1+m_1)\eta}}{\left(\lambda_1+m_1\right)m_1}+\frac{\lambda_1GcDAe^{(\lambda_1+m_2)\eta}}{\left(\lambda_1+m_2\right)m_2}\right)$$

$$+\frac{n_3}{n_2\left(n_3^2-n_2n_3\right)}\left(\frac{GrA^2e^{2\lambda_1\eta}}{2\left(\lambda_1-n_2\right)}+\frac{\lambda_1GrBAe^{(\lambda_1+\lambda_2)\eta}}{\left(\lambda_2-n_2\right)\left(\lambda_1+\lambda_2\right)}+\frac{\lambda_1GcCAe^{(\lambda_1+m_1)\eta}}{\left(m_1-n_2\right)\left(\lambda_1+m_1\right)}+\frac{\lambda_1GcDAe^{(\lambda_1+m_2)\eta}}{\left(m_2-n_2\right)\left(\lambda_1+m_2\right)}\right)$$

$$-\frac{1}{\left(n_3^2-n_2n_3\right)}\left(\frac{GrA^2e^{2\lambda_1\eta}}{2\left(\lambda_1-n_3\right)}+\frac{\lambda_1GrBAe^{(\lambda_1+\lambda_2)\eta}}{\left(\lambda_2-n_3\right)\left(\lambda_1+\lambda_2\right)}+\frac{\lambda_1GcCAe^{(\lambda_1+m_1)\eta}}{\left(m_1-n_3\right)\left(\lambda_1+m_1\right)}+\frac{\lambda_1GcDAe^{(\lambda_1+m_2)\eta}}{\left(m_2-n_3\right)\left(\lambda_1+m_2\right)}\right)\quad]$$

$$+...\quad-Gc\left\{\frac{R_1e^{m_1\eta}}{m_1}+\frac{R_2e^{m_2\eta}}{m_2}+\frac{Sc}{\left(m_2-m_1\right)}\left[\frac{m_1FCe^{(m_1+n_2)\eta}}{\left(m_1+n_2\right)}+\frac{m_1GCe^{(m_1+n_3)\eta}}{\left(m_1+n_3\right)}\right.\right.+$$

$$\left(\frac{n_3}{n_2\left(n_3^2-n_2n_3\right)}-\frac{1}{\left(n_3^2-n_2n_3\right)}\right)\left(\frac{m_1GrACe^{\left(m_1+\lambda_1\right)\eta}}{\lambda_1\left(m_1+\lambda_1\right)}+\frac{m_1GrBCe^{\left(m_1+\lambda_1\right)\eta}}{\lambda_2\left(m_1+\lambda_1\right)}+\frac{GcC^2e^{2m_1\eta}}{2m_1}+\frac{m_1GcDCe^{\left(m_1+m_2\right)\eta}}{m_2\left(m_1+m_2\right)}\right)$$

$$-\frac{n_3}{n_2\left(n_3^2-n_2n_3\right)}\left(\frac{m_1GrACe^{\left(m_1+\lambda_1\right)\eta}}{\left(\lambda_1-n_2\right)\left(m_1+\lambda_1\right)}+\frac{m_1GrBCe^{\left(m_1+\lambda_2\right)\eta}}{\left(\lambda_2-n_2\right)\left(m_1+\lambda_2\right)}+\frac{GcC^2e^{2m_1\eta}}{\left(m_1-n_2\right)2}+\frac{m_1GcDCe^{\left(m_1+m_2\right)\eta}}{\left(m_2-n_2\right)\left(m_1+m_2\right)}\right)$$

$$-\frac{1}{\left(n_3^2-n_2n_3\right)}\left(\frac{m_1GrACe^{(m_1+\lambda_1)\eta}}{\left(\lambda_1-n_3\right)\left(m_1+\lambda_1\right)}+\frac{m_1GrBCe^{(m_1+\lambda_2)\eta}}{\left(\lambda_2-n_3\right)\left(m_1+\lambda_2\right)}+\frac{GcC^2e^{2m_1\eta}}{\left(m_1-n_3\right)2}+\frac{m_1GcDCe^{(m_1+m_2)\eta}}{\left(m_2-n_3\right)\left(m_1+m_2\right)}\right)\quad]$$

$$+...]\}$$

$$E=0\qquad\qquad F=\frac{\left(f_{o(p)}\left(0\right)e^{-(\mu_3+1/2)}-f_{o(p)}\left(1\right)\right)e^{1/2}}{2\sinh\mu_3},$$

$$G = \frac{-\left(f_{o(p)}(0)e^{-(\mu_3+1/2)} - f_{o(p)}(1) \right)e^{1/2}}{2\sinh\mu_3} - f_{o(p)}(0)$$

$$J_1 = \frac{e^{\alpha x/2}\left(\gamma_1\Theta_w - \Theta_{1(p)}(\alpha x) + \Theta_{1(p)}(0)e^{-(\mu_1+1/2)\alpha x} \right)}{2\sinh(\mu_1\alpha x)} \quad,$$

$$J_2 = \frac{-e^{\alpha x/2}\left(\gamma_1\Theta_w - \Theta_{1(p)}(\alpha x) + \Theta_{1(p)}(0)e^{-(\mu_1+1/2)\alpha x} \right)}{2\sinh(\mu_1\alpha x)} - \Theta_{1(p)}(0)$$

$$R_1 = \frac{e^{\alpha x/2}\left(\gamma_2\Phi_w - \Phi_{1(p)}(\alpha x) + \Phi_{1(p)}(0)e^{-(\mu_2+1/2)\alpha x} \right)}{2\sinh(\mu_2\alpha x)} \quad,$$

$$R_2 = \frac{-e^{\alpha x/2}\left(\gamma_2\Phi_w - \Phi_{1(p)}(\alpha x) + \Phi_{1(p)}(0)e^{-(\mu_2+1/2)\alpha x} \right)}{2\sinh(\mu_2\alpha x)} - \Phi_{1(p)}(0)$$